

**DEEP OCEAN CIRCULATION CHANGES ACROSS THE  
MID-PLEISTOCENE TRANSITION**

by

Emily Symes

A thesis submitted to the Faculty of the University of Delaware in partial fulfillment of the requirements for the degree of Master of Science in Geology

Summer 2023

© 2023 Symes  
All Rights Reserved

**DEEP OCEAN CIRCULATION CHANGES DURING THE MID-  
PLEISTOCENE TRANSITION**

by

Emily Symes

Approved: \_\_\_\_\_  
Chandranath Basak, Ph.D.  
Professor in charge of thesis on behalf of the Advisory Committee

Approved: \_\_\_\_\_  
John A. Madsen, Ph.D.  
Chair of the Department of Earth Sciences

Approved: \_\_\_\_\_  
Fabrice Veron, Ph.D.  
Dean of the College of Earth, Ocean, and Environment

Approved: \_\_\_\_\_  
Louis F. Rossi, Ph.D.  
Vice Provost for Graduate and Professional Education and  
Dean of the Graduate College

## ACKNOWLEDGMENTS

I'd like to thank a number of people who supported and helped me through my master's journey. This period has truly been a cycle of ups and downs, personal growth, but also hardship and completing my thesis would not have been possible without the support of those around me. First, I'd like to thank my advisor, Chandranath Basak, for taking me on as a graduate student. Prior to meeting Chandranath and working in the BLOG lab, I had never thought about getting a graduate degree, so I am grateful for Chandranath for giving me the opportunity and for all his support during the program. I'd also like to thank my lab mates, Isuri Kapuge and Laura Johnson for their help with preparing and running some of the samples included in this thesis. I'd like to thank the members of IODP expedition 383 for collecting the samples that made this project possible and the additional faculty and staff that helped me along the way.

I'd especially like to thank my friends and family who have been my rocks through this period of my life. I'd like to thank my mom, Elizabeth Manley, for always believing I was capable and my Aunt, Barbara Manley for all of her guidance regarding my thesis and defense. I'd especially like to thank the graduate community here in the Geology department. Our daily lunch hours, weekly happy hours and fun get togethers have become something I cherish. I am so glad I got to call this department home for two years because I couldn't have asked for a more supportive bunch of students. I'd like to thank Lizz Whitney for our weekly walks that helped me destress after a long day of research and all the other friends I have made throughout

my time in the program. Finally, I would like to thank Lauren O'Connor for her support and for helping me through many stressful days and sleepless nights.

## TABLE OF CONTENTS

LIST OF FIGURES .....	vi
ABSTRACT .....	viii
Chapter	
1 INTRODUCTION.....	1
2 BACKGROUND.....	6
2.1 Study Area and Hydrography .....	6
2.2 Hypotheses Proposed to Explain the Mid-Pleistocene Transition .....	9
2.3 Global Ocean Circulation .....	10
2.4 Southern Ocean Circulation .....	14
2.5 The role of Deep Ocean Circulation on Climate .....	16
2.6 Neodymium Isotopes.....	17
2.6.1 Neodymium Isotopes as a Water Mass Tracer .....	17
2.6.2 Neodymium Isotopes in Marine Archives.....	19
3 METHODS.....	21
3.1 Analytical Details .....	21
3.2 Age Model.....	22
4 RESULTS.....	24
5 DISCUSSION.....	27
5.1 $\epsilon_{Nd}$ and the Mid-Pleistocene Transition.....	27
5.2 Global vs. Local Record .....	32
5.3 The $\epsilon_{Nd}$ and $\delta^{18}O$ records .....	34
5.4 North vs. South Control.....	36
CONCLUSIONS .....	40
REFERENCES .....	43

## LIST OF FIGURES

- Figure 1.1. Global benthic  $\delta^{18}O_{calcite}$ [‰] stacks covering the Mid-Pleistocene Transition. (a) Benthic oxygen isotope stack (Ahn et al., 2017) for the past 5000 ky (5 my) showing how the early oxygen isotope record differs from the Mid-Pleistocene Transition. (b) A close up of the benthic oxygen isotope stack (Ahn et al., 2017) showing just the study period (1500-500 ka). The boundaries of the Mid-Pleistocene Transition are indicated by the blue line on both panels. .... 2
- Figure 2.1: Location of study site U1541 and additional cores from IODP expedition 383. Red lines are Sub-Antarctic Front (SAF), and Polar front (PF) (Orsi et al., 1995). Figure made with Ocean Data View (<https://odv.awi.de/>)..... 7
- Figure 2.2: Depth profile of dissolved oxygen (ml/l) along the black line as shown in Fig. 1. Colors indicate dissolved oxygen concentrations and contours indicate salinity. Red-filled circles indicate the location of sites from expedition 383. NPDW = North Pacific Deep Water; LCDW = Lower Circumpolar Deep Water; AABW = Antarctic Bottom Water. .... 8
- Figure 2.3: Schematics of global overturning circulation. (a) The ocean conveyor belt as proposed by Broecker (1987). The red graphic indicates warm shallow currents and blue, cold and saline, deep currents from Tillinger, 2011.(b) A more detailed schematic of global overturning circulation. Purple (upper ocean and thermocline), red (intermediate water), orange (IDW and PDW), green (NADW), blue (AABW), gray (Mediterranean and Red Sea outflows) from Talley, 2013. .... 12
- Figure 2.4: Schematic showing general ocean circulation in the Southern Ocean. Water masses, corresponding abbreviations and line color are given in the key at the right of the schematic. Arrows indicate the direction of water mass movement. From Talley et al., 2011..... 15

Figure 4.1:  $\epsilon_{Nd}$  time series for Site U1541 spanning 500-1500 ka. The blue and black broken lines represent the modern ocean dissolved Nd isotope and most radiogenic value in the time series respectively. The blue dots represent the boundary of marine isotope stages (after Lisiecki and Raymo, 2005). The vertical grey bars and the numerals are the interglacial and glacial periods respectively. Core gap is shown as broken line. Measurement uncertainties ( $2\sigma$ ) are shown by vertical errors bars. .... 25

Figure 5.1: Proxy compilation showing changes in ice sheet, caloric summer energy, and global deep ocean circulation covering the Mid-Pleistocene Transition. (a) Benthic oxygen isotope stack (Ahn et al., 2017) showing a glacial periodicity of 41 kyr during the early Pleistocene, which transitioned into glacial recurrence every 100 kyr in the late Pleistocene. (b) Solar insolation peak calculated from caloric summer energy (after Tzedakis et al., 2017). The filled blue and red circles indicate insolation maxima, indicating glacial and interglacial periods, respectively. (c) Downcore  $\epsilon_{Nd}$  record from Site U1541 in the central South Pacific. The broken black line represents the most radiogenic value reached in the record. Measurement uncertainties ( $2\sigma$ ) are shown by vertical error bars. .... 31

Figure 5.2: Comparison between North Atlantic (ODP 607) and South Pacific (U1541)  $\epsilon_{Nd}$  timeseries for covering 500-1500 ka. The grey bars and marine isotope stages represent the interglacial and glacial respectively. Core gap is shown as broken line. Measurement uncertainties ( $2\sigma$ ) are shown by vertical errors bars. .... 34

Figure 5.3: Proxy compilation showing  $\delta^{18}O$  compared to Nd isotopes for site U1541. a) Global benthic  $\delta^{18}O_{calcite}[\text{‰}]$  stack (Ahn et al., 2017) and b) Benthic  $\delta^{18}O_{sw}$  record from the South Atlantic Ocean (modified from Elderfield et al., 2012). Both with Nd isotopes ( $\epsilon_{Nd}$ , red). C) A linear model showing the correlation between  $\delta^{18}O_{sw}$  and  $\epsilon_{Nd}$ . .... 35

Figure 5.4: South Pacific  $\epsilon_{Nd}$  and flux of Ice Rafted Debris (U1539, shipboard data, Winckler et al., 2021) for 500-1500 ka. The grey bars and marine isotope stages represent the interglacial and glacial respectively. Core gap is shown as broken line. Measurement uncertainties ( $2\sigma$ ) are shown by vertical errors bars. Black dots are boundaries of Marine Isotope Stages (Lisiecki and Raymo, 2005). .... 39

## ABSTRACT

The Mid-Pleistocene Transition (MPT), occurring between ~1250 to 700 Ka (1.25 to 0.7 Ma) marks a fundamental change in Earth's climate system when the glacial cyclicity of Earth changed from 41 to 100 Kyr. This observed change occurred independently of changes in solar insolation suggesting changing internal climate dynamics might have driven the transition. The South Pacific represents the largest fraction of the Southern Ocean and hence an important target region for studying internal climate dynamics during the MPT. Here, we use sediment core U1541 (54°13'S, 125°25'W, 3604 m) collected during the International Ocean Discovery Program (IODP) Expedition 383 to investigate changes in deep ocean circulation and the role of these changes played in solidifying the conditions of the MPT.

In this thesis, we present an authigenic Nd isotope (expressed as  $\epsilon_{Nd}$ ) time series from Site U1541 from 1500 – 500 ka.  $\epsilon_{Nd}$  shifts can be interpreted as tracking changes in the mixing proportions of two water mass end members, unradiogenic Atlantic ( $\epsilon_{Nd} \sim -13.5$ ) and radiogenic Pacific sourced waters (PSW,  $\epsilon_{Nd} \sim -4$ ). In our record, the proportions of water mass end members fluctuate across climate cycles with glacial cycles reflecting more Pacific source water, indicative of weakened Meridional Overturning Circulation (MOC). Across the MPT, we have observed three periods of increased PSW influence at ~1250 ka (MIS 38), ~900 ka (MIS 22), and ~650 ka (MIS 16) interpreted as periods of a more complete breakdown in MOC than

other glacials. The ~1250 ka event predates previous research suggesting ~900 ka was the first event of such magnitude. Comparison of our results with the ice volume (using  $\delta^{18}\text{O}_{\text{sw}}$ , a direct proxy of ice volume or sea level change) record for ODP 1123 (Elderfield et al., 2012) shows there is a strong correlation between the deep ocean circulation changes observed and global ice volume suggesting there is a mechanistic link between the two variables. We propose this link is a shift in the nature of Antarctic glaciers from terrestrial sourced to glaciomarine. The influx of freshwater into the surrounding oceans from melting glaciomarine glaciers near the Sub-Antarctic front (SAF) has the potential to destabilize the water column producing perturbations in deep ocean circulation of the magnitude observed in our record. The MPT ocean circulation perturbations could have promoted increased drawdown in  $\text{CO}_2$  and ice growth to produce the 100 kyr cycles of the MPT.

## **Chapter 1**

### **INTRODUCTION**

The Mid-Pleistocene Transition (MPT) is a significant period in Earth's climate history because there was a fundamental change in how Earth's climate system operates. Through much of the Pleistocene epoch (2580 – 12 ka), Earth's climate has been punctuated by a cyclic pattern of warm and cold intervals, commonly referred to as glacial cycles. These cyclic climate variations are largely related to astronomically driven solar insolation, otherwise known as the Milankovitch cycles. The Milankovitch cycles were first identified by Serbian Geophysicist, Milutin Milankovitch in the early 1900's (Milankovitch, 1941). According to his theory, ice sheet growth and decay are paced by boreal summer insolation controlled by three cycles: obliquity, precession and eccentricity (Milankovitch, 1941; Berger et al., 1988; Ruddimen, 2013) where obliquity is the angle of tilt of the Earth away from the vertical axis which varies every ~41 kyr, eccentricity is the variation in the Earth's orbit from elliptical to circular that takes ~100 kyr, and precession is the wobbling motion of the Earth, similar to that of a top, that varies every 23 and 19 kyr. These periodicities are observed in Pleistocene paleoclimate records specifically the benthic oxygen isotope record (Hays et al., 1976).

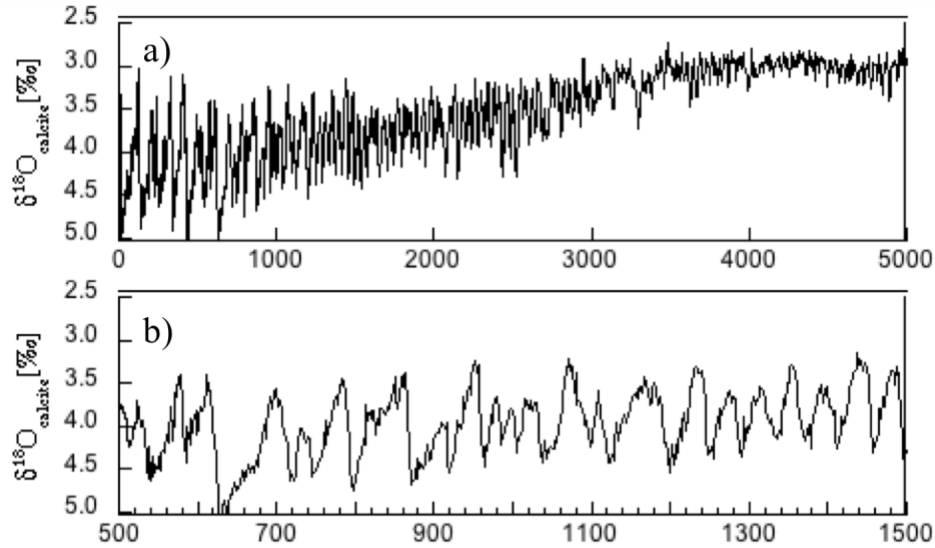


Figure 1.1. Global benthic  $\delta^{18}\text{O}_{\text{calcite}}$  [‰] stacks covering the Mid-Pleistocene Transition. (a) Benthic oxygen isotope stack (Ahn et al., 2017) for the past 5000 ky (5 my) showing how the early oxygen isotope record differs from the Mid-Pleistocene Transition. (b) A close up of the benthic oxygen isotope stack (Ahn et al., 2017) showing just the study period (1500-500 ka). The boundaries of the Mid-Pleistocene Transition are indicated by the blue line on both panels.

Throughout geologic history (55800 ka – 1250 ka), glaciers have appeared every 41 kyr. During this period, the glaciers were relatively small, and a warm phase (interglacial) that followed a cold phase (glacial period) would melt the majority of the glacier. During the MPT, occurring between 1250 ka and 700 ka, the dominant glacial recurrence interval changed from 41 kyr to 100 kyr and the glaciers were large enough that a large portion of ice volume remained during the interglacial with leftover ice entering into the subsequent glacial period, leading to larger glaciers. In the late Pleistocene (700 ka – present), this trend continued as the Earth entered a period

where glaciers consistently waxed and waned every 100 kyr and each glacial cycle witnessed a long period of ice growth (~90 kyr) and relatively fast deglaciation (~10 kyr) (Fig. 1.1).

The waxing and waning of early Pleistocene glaciers (i.e., ~41 kyr) have been shown to correspond predominately with variations in obliquity (i.e., 41 kyr). In contrast, glaciers of the late Pleistocene and MPT are not a function of changes in the Milankovitch cycles. This suggests that unlike conventional wisdom that proposes that the Milankovitch theory is the primary driver of Earth's cyclic climate variations, variations in the Milankovitch cycles alone cannot explain the shift from glacial waxing and waning occurring every 41 kyr in the early Pleistocene to 100 kyr in the late Pleistocene. Instead of being driven by variations in solar insolation, many scientists suggest that internal climate dynamics facilitated the changes of the MPT (Clark and Pollard, 1998; Lisiecki and Raymo, 2005; Clark et al., 2006; Elderfield et al., 2012; Pena & Goldstein, 2014, and many others).

Proposed mechanisms to explain the MPT range from long-term sea-surface and deep-water cooling (Huybers and Tziperman, 2008; Sosdian and Rosenthal, 2009), Southern and/or Northern Hemispheric sea-ice expansion (Lear et al, 2016), surface circulation changes in the North Atlantic (Poirier and Billups, 2014; Barker et al., 2021), declining atmospheric CO<sub>2</sub> (Chalk et al., 2017, Raymo et al., 1997; Hönisch et al., 2009), changes in Northern Hemisphere ice-sheet stability/dynamics (Clark et al., 2006; Snyder, 2016), and changes in deep ocean circulation (Pena and Goldstein, 2014; Farmer et al., 2019; Kim et al., 2020; Yehudai et al., 2021). Moreover, among

the potential drivers of MPT, a few are interlinked (e.g., atmospheric CO<sub>2</sub>, continental ice sheet dynamics, and deep ocean circulation) thereby complicating interpretation.

The MPT represents a period of time when climate records appear to have deviated from the expected patterns based on our current understanding of Milankovitch theory.

Therefore, it is evident that there are gaps in our understanding of Earth's climate system and how it operates. One hypothesis that has recently garnered much attention suggests that feedbacks between global deep ocean circulation and interactions with other climate components drove the MPT (Pena and Goldstein, 2014, Farmer et al., 2019, Kim et al., 2021, Yehudai et al., 2021). The majority of studies on deep ocean circulation across the MPT have focused on the North Atlantic sector while the Southern ocean has been minimally studied. Within the Southern Ocean the South Pacific is particularly understudied. The South Pacific, however, is an important region to study because it represents the largest volume fraction of the deep Southern Ocean and can act as a carbon reservoir that may store or release carbon on a glacial-interglacial time scale, therefore changes in deep ocean circulation evolution through time have global ramifications in relation to climate change making the region important for gaining a global perspective on deep ocean changes across the MPT.

This thesis aims to address the knowledge gap by providing critical data on Neodymium (Nd) isotopes, a well-recognized water mass tracer, for the South Pacific to further our understanding of how deep ocean circulation changed across the MPT and the role of the deep ocean circulation changes in the initiation of the MPT. The changes in deep ocean circulation will be interpreted in the context of changing

geochemical properties of deep ocean water masses, and ice-sheet dynamics off Antarctica and thereby add the South Pacific perspective to the current knowledge on pacing and development of MPT. The two hypotheses guiding this work are as follows:

1. *Deep ocean circulation changes during the Mid-Pleistocene Transition followed the Earth's climate pacing.*
2. *Global ice volume and deep ocean circulation are intrinsically linked and constitute parts of the non-linear feedback that facilitated the observed dominant frequency change during the MPT.*

## Chapter 2

### BACKGROUND

#### 2.1 Study Area and Hydrography

The study area is in the central South Pacific where sediment cores were collected during the International Ocean Discovery Program (IODP) Expedition 383 (Fig. 2.1). The IODP Exp. 383 recovered the first continuous sedimentary sections in the Sub- Antarctic Pacific Ocean with the potential to produce orbital-scale oceanographic records covering more than the last 2 Myr. IODP Site U1541 (54°13'S, 125°25'W, water depth 3604 m) is located ~300 km from the western flank of the East Pacific Rise (EPR). The site has an average sedimentation rate of ~3 cm/kyr. While multiple holes were drilled at Site U1541 to retrieve a continuous record, shipboard data (Lamy et al., 2019) show that a gap of ~1 meter (~ 40 kyr at about 1.1 Ma) is present.

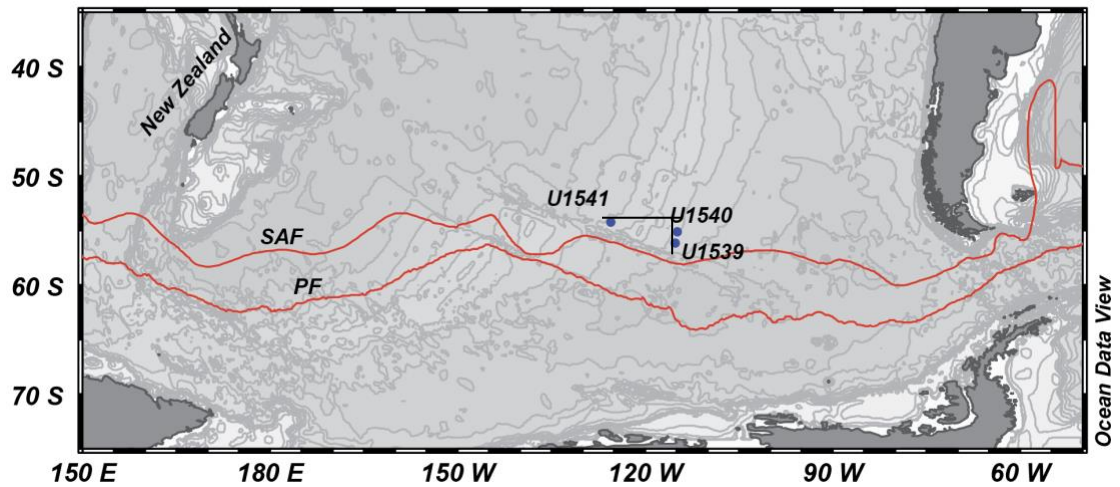


Figure 2.1: Location of study site U1541 and additional cores from IODP expedition 383. Red lines are Sub-Antarctic Front (SAF), and Polar front (PF) (Orsi et al., 1995). Figure made with Ocean Data View (<https://odv.awi.de/>).

Site U1541 also, sits at a water depth of 3604 m, approximately 185 km north of the Sub-Antarctic front (SAF), the outermost front of the Antarctic Circumpolar Current (ACC) (Fig. 2.1). Modern hydrography suggests that the modern location of Site U1541 is bathed by Lower Circumpolar Deep Water (LCDW) (Fig. 2.2, Lamy et al., 2019). The LCDW in the South Pacific is a remnant of saline North Atlantic Deep Water (NADW) (albeit modified) with a modest contribution from Antarctic Bottom Water (AABW) (Johnson, 2008) and North Pacific Deep Water (NPDW), a low oxygen water mass that often occupies depths between 1500 and 3500 m (Kawabe and Fujio, 2010).

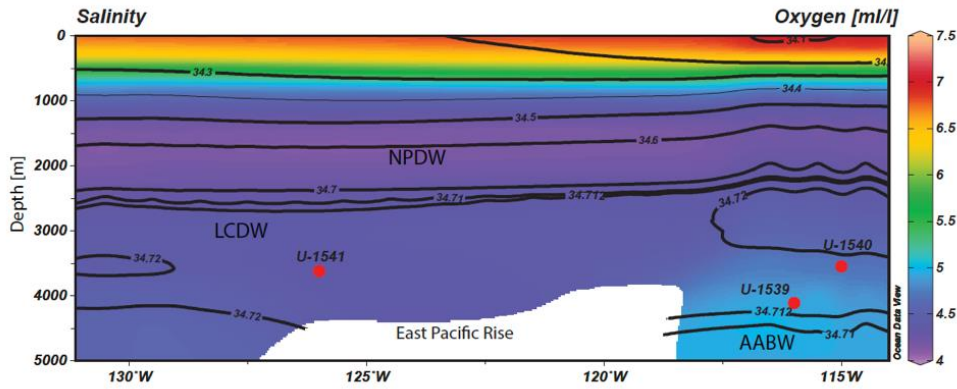


Figure 2.2: Depth profile of dissolved oxygen (ml/l) along the black line as shown in Fig. 1. Colors indicate dissolved oxygen concentrations and contours indicate salinity. Red-filled circles indicate the location of sites from expedition 383. NPDW = North Pacific Deep Water; LCDW = Lower Circumpolar Deep Water; AABW = Antarctic Bottom Water.

Site U1541 is well positioned to capture deep ocean circulation changes before, during, and after to Mid-Pleistocene Transition (MPT) by measuring the relative proportions of Atlantic (i.e., NADW) and Pacific (i.e., NPDW) sourced water masses in the South Pacific basin. Changes in deep ocean circulation have been tracked, in recent years, by utilizing Nd isotopes where changes in  $\epsilon_{Nd}$  have been thought to reflect these changes in mixing proportions. Most deep ocean circulation records across the MPT have been confined to the Atlantic sector of the oceans and are therefore dominated by NADW. The study site, on the other hand, is located in the central South Pacific at the far end of the global ocean circulation pathway and is therefore dominated by Pacific waters (i.e., AABW, NPDW) contributing more of a Pacific perspective to our understanding of how deep ocean circulation changed across the MPT. In addition, the Pacific sector of the Southern Ocean does not have a long-term Nd isotope record covering the MPT to contribute to this knowledge. A time

series Nd isotope record from U1541 can complement knowledge about the link between deep ocean circulation and the MPT that is emerging from Atlantic records (Pena and Goldstein, 2014, Kim et al., 2021, Farmer et al., 2019; Yehudai et al., 2021).

Site U1541 is also in the vicinity of areas that are important for the formation of deep (Ross Sea Bottom Water) and intermediate (Antarctic intermediate water) water masses (Fig. 2.1) with Ross Sea Bottom Water (RSBW) being an important contributor to the formation of AABW. The study site is also located near a significant region of ocean ventilation, where deep waters from the abyssal Southern Ocean upwell transporting stored and respired carbon into the surface oceans. Both the formation of new water masses and deep ocean ventilation are important aspects of global ocean circulation, the deep ocean's behavior and the associated carbon cycle.

## **2.2 Hypotheses Proposed to Explain the Mid-Pleistocene Transition**

Three mechanisms have been used to explain the Mid-Pleistocene Transition (MPT). These include ice sheet dynamics, long term global cooling related to carbon dioxide, and rearrangements in ocean circulation. The ice sheet feedbacks hypothesis was first proposed by Clark and Pollard (1998) where they proposed that thick layers of unconsolidated, rocky material, known as regolith, covered the continents, prior to the MPT. The regolith promoted the growth of thin yet wide reaching ice sheets that eroded the regolith away with each successive glaciation until crystalline bedrock was exposed. The crystalline bedrock promoted the growth of thick, high volume ice sheets. Clark and Pollard (1998) suggest that the exposure of the crystalline bedrock

corresponds to the start of the MPT and the presence of thicker, longer lasting ice sheets.

The second hypothesis proposes that declining atmospheric CO<sub>2</sub> (Willeit et al., 2019) promoted the growth of larger ice sheets that were capable of surviving initial deglaciation (Chalk et al., 2017, Raymo et al., 1997). The hypothesis of gradual decline in CO<sub>2</sub> is supported by some researchers however, this hypothesis is heavily contested with other scientists suggesting CO<sub>2</sub> levels remained similar to those of the early Pleistocene. Some researchers suggest the gradual lowering of CO<sub>2</sub> caused the MPT while other suggest CO<sub>2</sub> did not play a role in the MPT because CO<sub>2</sub> levels remained similar to where they have been historically (Honisch et al., 2009).

Among the commonly invoked hypotheses for explaining the MPT, the hypothesis that has garnered the most attention suggests that rearrangements in deep ocean circulation (Pena and Goldstein, 2014, Farmer et al., 2019, Kim et al., 2020, Yehudai et al., 2021) ushered by increases in global ice volume were an important mechanism in stabilizing the 100 ka ice sheets of the MPT. This hypothesis suggests that weakening of Meridonal Overturning circulation (MOC) across the MPT promoted deep ocean carbon storage, cooling and the formation of larger ice sheets.

### **2.3 Global Ocean Circulation**

Meridional Overturning Circulation (MOC), is a system that circulates North Atlantic and Antarctic Bottom waters through the global oceans. In the simplest form, MOC can be divided into two components; a surface and deep component that are connected through wind driven upwelling and downwelling. The surface component carries warm waters towards the poles where it downwells along continental coastlines and through increased density gradients. A deep component carries cold, deep waters

towards the equator, during the process they begin to upwell due to warming and the associated density decrease (Fig. 2.3). The MOC distributes heat, nutrients and dissolved gases around the globe and plays an important role in regulating Earth's climate.

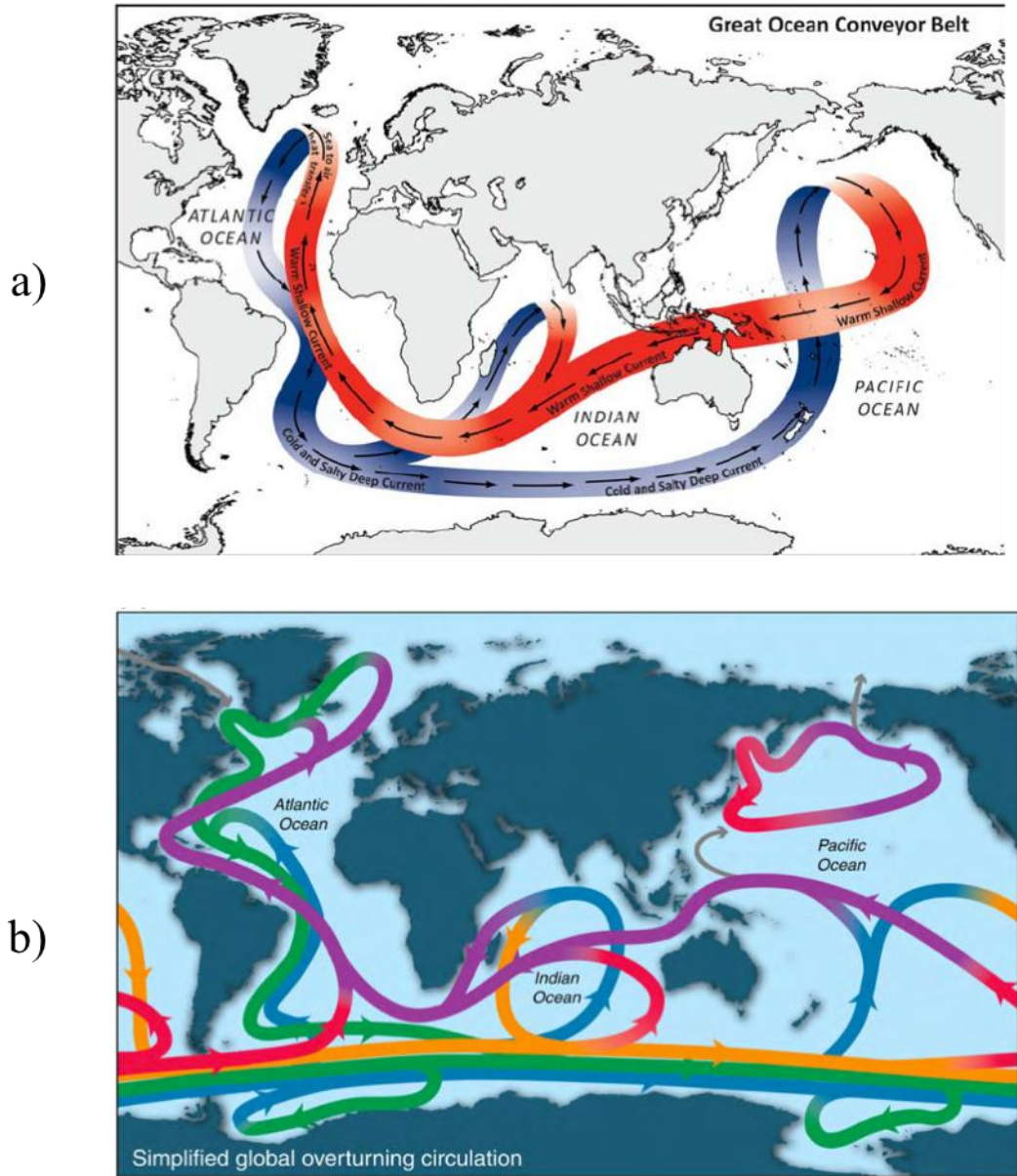


Figure 2.3: Schematics of global overturning circulation. (a) The ocean conveyor belt as proposed by Broecker (1987). The red graphic indicates warm shallow currents and blue, cold and saline, deep currents from Tillinger, 2011. (b) A more detailed schematic of global overturning circulation. Purple (upper ocean and thermocline), red (intermediate water), orange (IDW and PDW), green (NADW), blue (AABW), gray (Mediterranean and Red Sea outflows) from Talley, 2013.

The MOC, often recognized as the ‘Ocean conveyor belt’ (Fig. 2.3, b) is driven by the formation of deep water at high latitudes namely, North Atlantic Deep Water (NADW, Green) and Antarctic Bottom Water (AABW, Blue) with NADW being derived in the North Atlantic and AABW derived primarily in the Ross and Weddell seas off the coast of Antarctica. NADW and AABW represent the primary cold, deep components of the MOC system. The formation of NADW is complex with variable contributions from deep waters in the Nordic seas, Labrador seas and Mediterranean Overflow water (Talley, 2013). AABW forms when cold, surface waters (e.g. Sub-Antarctic mode water) combine with brine generated during sea ice formation in the Southern Ocean. Both northern and southern sourced deep waters are very cold, saline waters with high densities that sink to the abyssal oceans and flow in their opposing directions with NADW flowing South and AABW flowing north through the Atlantic. NADW and AABW move through the oceans and mix with other water masses through convection and mixing within the Antarctic Circumpolar Current (ACC). NADW and AABW are then incorporated into the production of altered water masses with different salinity and density properties than the source water mass. Along the ACC, wind driven upwelling brings some deep waters to the surface establishing a critical connection between the deep and surface oceans. During upwelling these water masses, once again undergo alterations through water mass mixing, advection and convection becoming surface and intermediate waters (i.e., AAIW, red) that encompass the warm, surface component of the MOC system. These surface waters move along the ocean surface eventually being reutilized in the formation of deep water, continuing the global MOC cycle. (Fig. 2.3, a,b)

## **2.4 Southern Ocean Circulation**

The Southern Ocean is broadly defined as the ring of water that encircles Antarctica. The ocean circulation in this region, on its own, is a complex process (Fig. 2.5). The upper waters of the Southern Ocean are unimpeded by continental boundaries promoting continuous, current flow around Antarctica. In contrast, deep Southern Ocean circulation is heavily controlled by ocean bathymetry in the region. As mentioned previously, the Southern Ocean is also the primary location of Antarctic Bottom Water formation (AABW), a key component of Meridional Overturning Circulation (MOC).

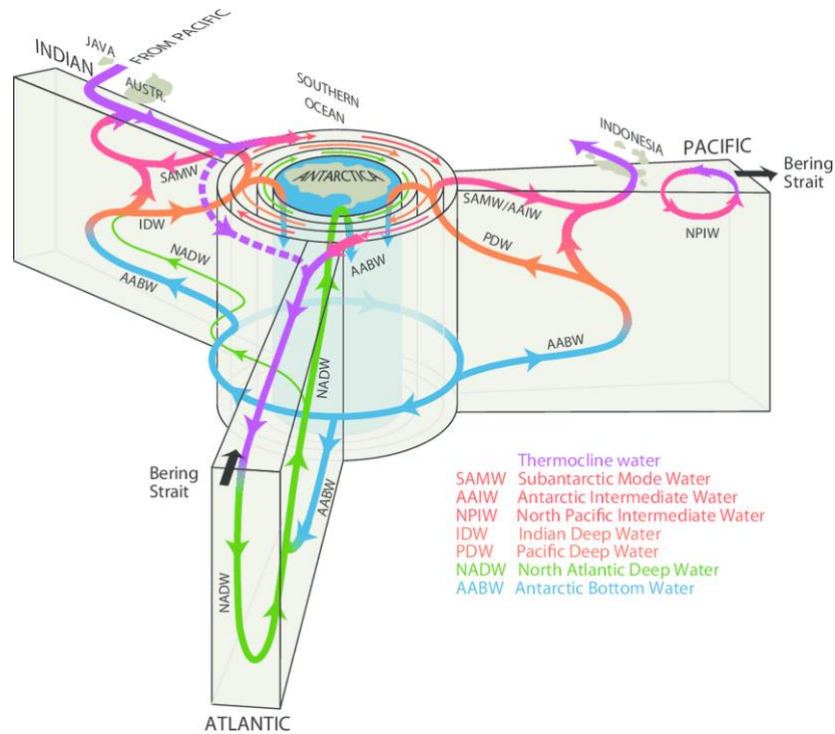


Figure 2.4: Schematic showing general ocean circulation in the Southern Ocean. Water masses, corresponding abbreviations and line color are given in the key at the right of the schematic. Arrows indicate the direction of water mass movement. From Talley et al., 2011.

Southern Ocean circulation has two primary components. First, AABW forms off the coast of Antarctica within the Ross and Weddell Seas moving northward into the Atlantic, Pacific and Indian oceans along the ocean floor at depths below 4000 meters (Talley et al., 2011). Second, the Southern Ocean is an important location of water mass mixing, alteration and redistribution through the Antarctic Circumpolar Current (ACC). The ACC is the primary current in the Southern Ocean and also one of the strongest currents on Earth. The ACC is a deep reaching current that flows eastward around Antarctica (Talley et al., 2011). Water masses from other ocean

basins including North Atlantic Deep Water (NADW) from the Atlantic, Pacific Deep Water (PDW) from the Pacific and Indian Deep Water (IDW) flow southwards where they are incorporated in the ACC (Fig. 2.4). Once incorporated in the ACC, these deep-water masses mix and are redistributed as new, altered water masses. These include Lower Circumpolar Deep Water (LCDW) primarily a product of NADW, with some contributions from AABW, PDW and IDW, Upper Circumpolar Deep Water (UCDW), a product of some combination of PDW and IDW and more AABW. In addition, water mass mixing in the ACC contributes to surface and intermediate water formation including the formation of Sub-Antarctic Mode Water (SAMW) and Antarctic Intermediate Water (AAIW). Intermediate and Surface waters ultimately contribute to new deep-water formation and the distribution of heat around the Earth. Not only is the Southern Ocean an important location of deep-water formation that drives MOC, but it is also an important location for the formation of other important ocean water masses involved in MOC and ultimately has strong implications on global climate.

## **2.5 The role of Deep Ocean Circulation on Climate**

The deep oceans play an important role in global climate regulation through carbon storage and exchange with the atmosphere. The oceans are the largest carbon reservoir that can exchange with the atmosphere at a thousand-year timescale. Of the carbon stored in the oceans, the largest proportion is stored in the deep oceans making it an important driver that controls Earth's climate.

While the Oceans' roles in carbon cycle is varied and complex, one of the primary conduits through which carbon makes it to the deep ocean is via biological pump, and remineralization. The surface-dwelling organisms utilize atmospheric CO<sub>2</sub> to produce biomass which eventually starts to sink through the water column into the deeper oceans where remineralization/respiration releases CO<sub>2</sub> into the ocean deep waters. Therefore, the deep ocean becomes a reservoir of carbon that can only be released into the atmosphere if the deep-water masses (i.e., NADW, AABW) come up to the surface and interact with the atmosphere through air-sea exchange. Deep ocean circulation is responsible for moving water masses around through the Meridional overturning circulation (MOC) process and hence is critical towards controlling this aspect of the carbon cycle.

## **2.6 Neodymium Isotopes**

### **2.6.1 Neodymium Isotopes as a Water Mass Tracer**

Nd isotopes can be used to trace present and past ocean circulation, because its variability in the earth mainly reflects the radioactive decay of <sup>147</sup>Sm to <sup>143</sup>Nd ( $t_{1/2} = 10^6$  Ga) over geological time, rather than temperature, redox, air-sea exchange, or biology. Sm/Nd ratios show a small variation in continental rocks and are low compared to the mantle. As a result, the continents have lower <sup>143</sup>Nd/<sup>144</sup>Nd values than the mantle, and there is a systematic relationship between Nd isotope ratios and crustal age, with the older continents having lower values. Nd isotopes are often presented as  $\epsilon_{Nd}$ , defined as the deviation of the <sup>143</sup>Nd/<sup>144</sup>Nd ratio in a sample from the average

value of chondritic uniform reservoir ( $=0.512638$ , Jacobsen and Wasserburg, 1980) in parts per  $10^4$ .

The average oceanic residence time of Nd is about 600-1200 yrs (Jeandel, 1993; Tachikawa et al., 1999), which is less than the average oceanic mixing time ( $\sim 1500$  yrs; Broecker and Peng, 1982). As a result of this characteristic, in the oceans,  $\epsilon_{Nd}$  values show systematic geographic variability that mirrors the age of the (older) continental sources of Nd in the North Atlantic (North Atlantic Deep Water, (NADW),  $\epsilon_{Nd} = \sim -13.5$ ) versus (young) mantle-derived volcanic material in the Pacific (North Pacific Deep Water, (NPDW),  $\epsilon_{Nd} = -4$ ). These end members have been shown to have remained constant over time (Pena and Goldstein, 2014). More recently, there have been some studies which claim to have additional non-conservative sources of Nd from the bottom sediments (Abbott et al., 2015a, b), however, the majority of open ocean observational studies are yet to support that new interpretive framework. Below the thermocline, in the modern ocean dissolved  $\epsilon_{Nd}$  measurements can be largely explained by water mass mixing (Wu et al., 2022). Particularly in the South Pacific, studies show that  $\epsilon_{Nd}$  behaves as a conservative tracer and can be reliably used to study water mass mixing (Carter et al., 2012; Rickli et al., 2014, Basak et al., 2015). Hence, in this thesis, I will follow the traditional interpretation which posits that measured  $\epsilon_{Nd}$  in a marine archive that represents dissolved seawater value can be explained as linear end member mixing between water masses.

### **2.6.2 Neodymium Isotopes in Marine Archives**

The archive was carefully selected to construct a time series of past seawater Nd isotopes. Fossilized bio-phosphate (fossil fish teeth/debris) is one of the best archives that faithfully records past seawater Nd isotope ratios, as they contain high Nd concentrations and are found throughout the global ocean (e.g., Martin and Haley, 2000). Nd is added to fossil fish teeth/debris soon after deposition when the teeth/debris are still in contact with bottom seawater at the sediment water interface (Wright et al., 1984; Shaw and Wasserburg, 1985; Martin and Haley, 2000). In constructing the seawater Nd isotope record I prioritized use of fossilized bio-phosphate.

Nd isotopes preserved in ferromanganese oxide precipitates in deep sea cores have been used to reconstruct MOC changes over the last ice age (e.g., Rutberg et al., 2000; Piotrowski et al., 2004, 2005, 2012; Gutjahr et al. 2008; Roberts et al. 2010; Kim et al., 2021, and many others). The approach is based on observations that Fe-Mn oxy-hydroxide coatings form in the lower water column and record the near-bottom seawater Nd isotopic signal (e.g., Palmer and Elderfield 1985; Albarède and Goldstein 1992). In the event that fossilized bio-phosphates were not available in my samples, I analyzed planktonic foraminifera, carefully separated from any detrital particles, to obtain the seawater Nd isotopic values from its Fe-Mn oxy-hydroxide coatings. Several core top studies have demonstrated that Nd isotopes from detritus-free “unclean” (Fe-Mn oxy-hydroxide encrusted) planktonic foraminifera faithfully record bottom water Nd isotopic signatures (e.g., Roberts et al., 2010, 2012; Elmore et al.,

2011; Wilson et al., 2012; Molina-Kescher et al., 2014).

## Chapter 3

### METHODS

#### 3.1 Analytical Details

Fossilized bio-phosphate (fossil fish teeth/debris) and Fe-Mn oxy-hydroxide encrusted planktonic foraminifera used for Nd isotope analyses were hand-picked (from the  $>63 \mu\text{m}$  fraction) under a microscope, followed by careful physical cleaning of detrital particles, which is critical for obtaining the pure paleo seawater signal. Physical cleaning typically comprised multiple rinses and sonication in Optima grade methanol, followed by multiple rinses in deionized water (e.g., Wilson et al., 2012; Pena et al., 2013). Although the basic steps were similar to previously published studies, this kind of protocol tends to evolve based on the sample in question. The foraminifera were crushed with glass slides to break open the inner chamber before proceeding with the physical cleaning. The cleaned broken foraminifera fragments were examined under a microscope to ensure that no clay fragments were left in the sample. The majority of samples used to generate the continuous record of  $\epsilon_{\text{Nd}}$  were fish teeth because it is widely accepted that fossil fish teeth are the most reliable recorders of paleo seawater. Where fish teeth were not available, foraminifera were used instead.

After the physical cleaning, the fossil fish teeth/debris were subjected to dissolution using aqua regia and the foraminifera using 5% acetic acid. Rare earth

element separation uses 100  $\mu\text{L}$  shrink fit Teflon columns, loaded with Eichrom TRUspec resin (100–150  $\mu\text{m}$  mesh). Further isolation of Nd uses calibrated Teflon columns pre-loaded with Eichrom LNspec resin (50-100  $\mu\text{m}$  mesh). Samples were analyzed on the ThermoScientific Neptune Plus multi-collector inductively coupled plasma mass-spectrometer (MC-ICPMS) at Pennsylvania State University (PSU), where samples as small as 15-20 ng total Nd are now routinely measured for  $\epsilon_{\text{Nd}}$ . Recent analyses by our group of 20 ng international standard JNdi yielded reproducibility of  $\pm 0.30 \epsilon_{\text{Nd}}$  units ( $2\sigma$ ,  $n=19$ ).

### 3.2 Age Model

The U1541 age model used in this study was generated by aligning high-resolution benthic  $\delta^{18}\text{O}$  with the probabilistic stack (hereafter Prob-Stack) using the Hidden Markov Model (HMM) algorithm of Lin et al. (2014) and Ahn et al. (2017). The U1541 oxygen isotope record was generated using a combination of *C. kullenbergi* and *C. wuellerstorfi* foraminifera (Middleton, Winckler, and Gottschalk, *personal communications*). The Prob-Stack has been used as a reference record as it contains a total of 180 globally distributed benthic  $\delta^{18}\text{O}$  records. The Prob-Stack is a marked improvement over the most widely used LR04 stack (Lisiecki and Raymo, 2005) because it contains 123 more benthic  $\delta^{18}\text{O}$  records that are also well distributed across latitude, longitude, and depth. Besides, the HMM match algorithm allows to calculate and report uncertainties in the alignments. This age model has been

developed by a sub-set of expedition 383 shipboard scientists and agreed upon to be used for all subsequent publications for Site U1541 (Lamy et al., 2021).

## Chapter 4

### RESULTS

A total of 84 samples were analyzed for Nd isotopes from Site U1541 to generate a downcore record spanning 500-1500 ka with variable sampling resolution mostly around  $\sim$  a sample/20 kyr. Throughout the record, the  $\epsilon_{Nd}$  values oscillated between -5.5 and -8 with semi-regular cyclicity, following the pacing of the initiation and termination of glacial intervals (Fig. 4.1, shaded boxes represent interglacial periods). The broken blue and black lines in Fig 4.1 indicate the modern ocean measured  $\epsilon_{Nd}$  at Site U1541 (Basak et al., 2015) and the most radiogenic value observed in the entire record. Throughout the record, glacial periods display more radiogenic  $\epsilon_{Nd}$  values than interglacial periods and these values periodically fluctuate between more and less radiogenic values. Interglacial values typically approach the modern day dissolved  $\epsilon_{Nd}$  value at Site U1541 of  $\sim$ -7.6 (Basak et al., 2015), while glacial values vary over similar timescales. Fluctuations in  $\epsilon_{Nd}$  across both glacial and interglacial periods vary between the pre-MPT (1500-1250 ka), MPT (1250 – 700 ka), and post-MPT (700-500 ka).

In the pre-MPT (1500-1250 ka), interglacial values reach the modern day dissolved  $\epsilon_{Nd}$  value less often than during and after the MPT. There is also a shift towards more radiogenic  $\epsilon_{Nd}$  values during glacials. Beginning around 1400 ka, there

is a general trend in  $\epsilon_{Nd}$  towards increasingly radiogenic  $\epsilon_{Nd}$  values with each consecutive glacial until reaching the most radiogenic value of -5.67 at MIS 38 (~1250 ka). In addition, the pre-MPT record shows a change in  $\epsilon_{Nd}$  of  $\sim$ -1 between each glacial and consecutive interglacial.

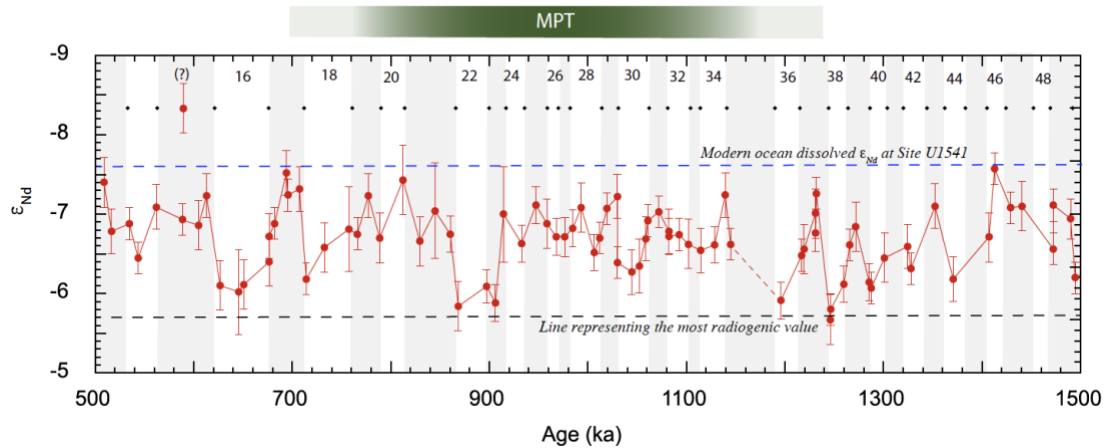


Figure 4.1:  $\epsilon_{Nd}$  time series for Site U1541 spanning 500-1500 ka. The blue and black broken lines represent the modern ocean dissolved Nd isotope and most radiogenic value in the time series respectively. The blue dots represent the boundary of marine isotope stages (after Lisiecki and Raymo, 2005). The vertical grey bars and the numerals are the interglacial and glacial periods respectively. Core gap is shown as broken line. Measurement uncertainties ( $2\sigma$ ) are shown by vertical errors bars.

During the Mid-Pleistocene Transition (MPT) (1250 -700 ka)  $\epsilon_{Nd}$  values continue to fluctuate between glacial and interglacial periods however, the amplitude of change in between consecutive glacial and interglacial is smaller ( $\epsilon_{Nd} \sim$ -0.50) than the Pre-MPT. There is a second, strong radiogenic excursion during MIS 22 (900 ka), reaching a value of -5.88.

In the post-MPT (700-500 ka)  $\epsilon_{Nd}$  values fluctuate similarly to the previous two periods broadly following the same oscillatory pattern with a variation in amplitude across consecutive glacial and interglacial periods around  $\sim 1$ , similar to that of the Pre-MPT. There is a third prominent radiogenic excursion during MIS 16 (650 ka) around  $\epsilon_{Nd} \sim -6$  (Fig. 4.1).

In summary,  $\epsilon_{Nd}$  values fluctuate with Earth's climate cycles with more radiogenic values occurring during glacial periods. There are three strong radiogenic excursions throughout the record which have above average  $\epsilon_{Nd}$  values compared to the remainder of the dataset. MIS 38 has the most radiogenic values of the entire data set which is a surprising finding because this period is not a prolonged or more extreme glacial interval based on the  $\delta^{18}O$  record. In addition, the change  $\epsilon_{Nd}$  amplitude across the MPT is an interesting finding because these changes are also not reflected in the  $\delta^{18}O$  record.

## Chapter 5

### DISCUSSION

#### 5.1 $\epsilon_{Nd}$ and the Mid-Pleistocene Transition

Early reviews of the climatic changes that happened during the Mid-Pleistocene Transition (MPT) placed the MPT from ~1250 ka to 700 ka (Clark et al., 2006). Since the deep ocean can act as a critical carbon reservoir on a multi-millennial timescale, the role of deep ocean circulation and how it changed over the MPT has always been a central topic of palaeoceanographic discussions. While  $\delta^{13}C$  has been the conventional proxy used to study past changes in deep ocean circulation (e.g., Shackleton, 1977; Raymo et al., 1990, 2004; Mix et al., 1995), using Nd isotopes as a water mass tracer has recently gained popularity to study changes in deep ocean circulation during the MPT (Pena and Goldstein, 2014; Farmer et al., 2019; Kim et al., 2021; Yehudai et al., 2021).

The conservative nature, residence time and geographic variability of Nd isotopes make  $\epsilon_{Nd}$  a reliable water mass tracer (Goldstein and Hemming, 2003; Ivan De Flierdt et al., 2016, and many others) for studying water mass mixing.  $\epsilon_{Nd}$  in marine archives can therefore reliably be used to track changes in deep ocean end member mixing. The traditional interpretation suggests that  $\epsilon_{Nd}$  in marine archives

reflects changes in end member mixing of Atlantic (i.e., NADW,  $\epsilon_{Nd} \sim -13.5$ ) sourced waters and Pacific (i.e., NPDW,  $\epsilon_{Nd} \sim -4$ ) sourced waters (Fig. 5.1). Following this interpretation, the more radiogenic values in the Nd isotope record for Site U1541 reflect greater Pacific water end member prevalence or less Atlantic water export to the region. More radiogenic values are consistently observed during glacial periods throughout the Nd isotope record for Site U1541 (Fig. 5.1) suggesting increased Pacific water prevalence across glacial periods. The opposite is also true suggesting decreased Atlantic water export instead. The more radiogenic values across glacial periods are also thought to reflect periods of weakened Meridional Overturning Circulation (MOC) through the global oceans (Pena and Goldstein, 2014, Yehudai et al., 2019).

While these cyclic shifts from more radiogenic  $\epsilon_{Nd}$  values are common throughout the entire Nd isotope record for Site U1541, our record for the South Pacific reveals three periods with higher than average radiogenic values during MIS 38 (~1250 ka), MIS 22 (900 ka), and MIS 16 (650 ka). These periods contain the most radiogenic values found in the entire Nd isotope record. MIS 22 occurring around ~900 ka is often considered the first significant period of almost complete breakdown in MOC, believed to have played a significant role in triggering and solidifying the 100 kyr cycles and conditions of the MPT. Elderfield et al., (2012) showed, based on seawater  $\delta^{18}O$  records from the Chatham rise in the South Pacific, that the first major large continental ice growth of the MPT occurred during MIS 22. Pena and Goldstein

(2014) found MIS 22 to be equally as significant showing there were significant changes in deep ocean circulation MIS 22, in addition to major changes in continental ice growth. They coined the term “AMOC Crisis” to describe deep ocean circulation changes that occurred during MIS 22. Based on these studies, it is fair to claim that MIS 22 is a landmark time interval that led to the 100 kyr interglacial-glacial pacing of the late Pleistocene.

Our Nd isotope record (Fig. 4.1) is the first continuous Nd isotope record in the central South Pacific that encompasses the entire range of the MPT. Our record shows two other prominent radiogenic  $\epsilon_{Nd}$  excursions like the one at MIS 22. With radiogenic excursions at MIS 38 (~1250 ka) and another around MIS 16 (~650 ka). Of the three excursions, MIS 38 has the most radiogenic values reaching  $\epsilon_{Nd} = -5.8$ . The  $\epsilon_{Nd}$  excursion at ~ MIS 38 (~1250 ka) occurs gradually, following three smaller excursions showing a gradual shift towards more radiogenic values with each consecutive glacial, beginning around 1400 ka. Therefore, if we consider the  $\epsilon_{Nd}$  excursion at ~900 ka to represent a complete breakdown in deep ocean circulation as suggested by Pena and Goldstein (2014), then the new dataset presented in this thesis suggests that similar events happened prior to 900 ka at 1250 ka. This is supported by the work of Tzedakis et al. (2017) showing that the first time an ice sheet survived a significant melting event during an insolation peak happened much earlier in the MPT than 900 ka.

Tzedakis et al. (2017) used an integrated Northern Hemisphere summer insolation and a time-dependent discount metric to calculate the amount of insolation required to produce an interglacial. This model allowed the authors to classify the insolation maxima into three categories: one that is associated with the onset of an interglacial (Figure 5.1, filled red circles), one that is associated with continued interglacial (Figure 5.1, empty blue circles), and the third is interstadials (Figure 5.1, filled blue circles). Based on this classification, interglacials happened every other insolation peak prior to 1250 ka. However, after 1250 ka, deglaciation started happening every two or more insolation peaks, perhaps indicating the increase in ice sheet that could survive consecutive insolation peaks. This inferred ice sheet growth and climate response is also in agreement with the timing of major MOC perturbation as observed in the  $\epsilon_{Nd}$  record  $\sim$ 1250 ka. The Nd isotope record and work of Tedakis et al., (2017) suggests that 1250 ka is an important time period in Earth's history when significant changes happened in the climate realm, ushering in the 100 Kyr late Pleistocene interglacial-glacial pattern. In addition, the cooccurrence of these MOC perturbations with the onset of larger glaciations capable of surviving the following insolation maximum (Tedakis et al., 2017) suggests there is a mechanistic link between deep ocean circulation and ice volume across the MPT.

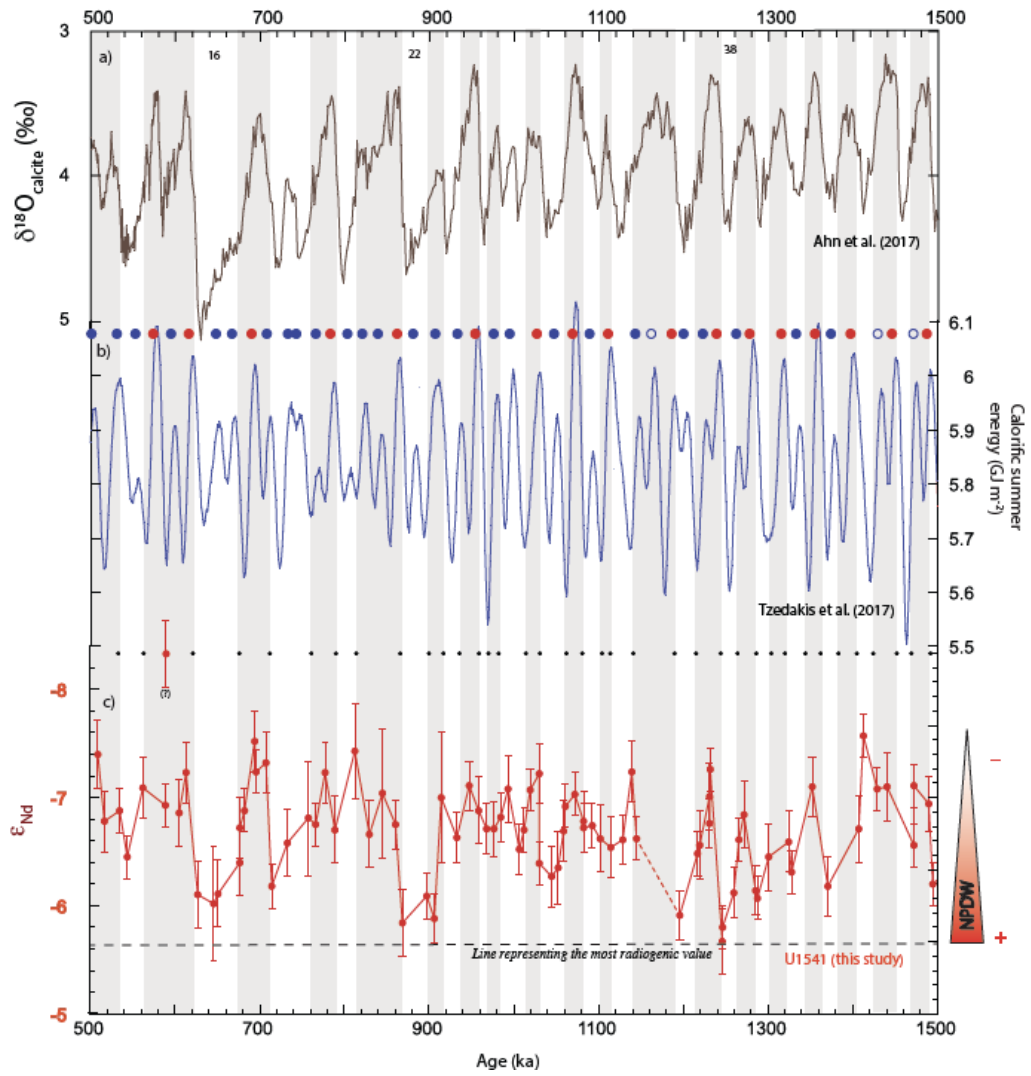


Figure 5.1: Proxy compilation showing changes in ice sheet, caloric summer energy, and global deep ocean circulation covering the Mid-Pleistocene Transition. (a) Benthic oxygen isotope stack (Ahn et al., 2017) showing a glacial periodicity of 41 kyr during the early Pleistocene, which transitioned into glacial recurrence every 100 kyr in the late Pleistocene. (b) Solar insolation peak calculated from caloric summer energy (after Tzedakis et al., 2017). The filled blue and red circles indicate insolation maxima, indicating glacial and interglacial periods, respectively. (c) Downcore  $\epsilon_{\text{Nd}}$  record from Site U1541 in the central South Pacific. The broken black line represents the most radiogenic value reached in the record. Measurement uncertainties ( $2\sigma$ ) are shown by vertical error bars.

## 5.2 Global vs. Local Record

There are three periods in the U1541  $\epsilon_{Nd}$  record that stand out as having above-average radiogenic  $\epsilon_{Nd}$  values. These occur during Marine Isotope Stages (MIS) 38 (~1250 ka), MIS 22 (~900 ka), and MIS 16 (~650 ka) (Figure 5.3), with corresponding highest  $\epsilon_{Nd}$  values of  $-5.80 \pm 0.20$ ,  $-5.84 \pm 0.23$ , and  $-6.02 \pm 0.53$ , respectively. All three peaks are defined by values that are within error of each other and are therefore statistically similar. A comparison with the North Atlantic record from ODP 607 (Kim et al., 2021) shows that similar three radiogenic excursions are also present during MIS 16, 22, and 36 (Figure 5.2). The overall agreement between the South Pacific and North Atlantic records is excellent, in that the smaller features such as the three preceding radiogenic excursions beginning around 1400 ka and leading up to the 1250 ka peak are observed in both records. Therefore, the U1541  $\epsilon_{Nd}$  timeseries can be claimed to have captured the global deep ocean circulation changes during the Mid-Pleistocene Transition (MPT).

While the similarities between the South Pacific and North Atlantic are quite remarkable, there are also differences and mismatches that provide additional information linked to basin-scale changes on top of the global signal. For example, at all three excursions discussed above, the magnitude of change in  $\epsilon_{Nd}$  is ~3 and ~1 epsilon unit in the North Atlantic and South Pacific, respectively. This difference in magnitude of change can be explained by the respective locations of the sites in question. Site 607 in the North Atlantic is located close to where the North Atlantic

Deep Water (NADW) with its signature  $\epsilon_{Nd}$  values of -13.5 is being formed. To explain the  $\epsilon_{Nd}$  excursions in the record, if we invoke reorganization of deep ocean circulation that involves slowing down or stopping of NADW, then owing to its location in the vicinity of NADW formation, Site 607 would have undergone a large change in  $\epsilon_{Nd}$  as the primary unradiogenic source is cut off. In contrast, U1541, which is far from the area of NADW formation, receives residual NADW that is heavily modified with a likely  $\epsilon_{Nd}$  value of -9 to -10 by the time it enters the Pacific (Molina Kescher et al., 2014). Therefore, the  $\epsilon_{Nd}$  signature of NADW in the North Atlantic and South Pacific are fundamentally different and thus in a state when NADW is reduced, the changes that will likely be reflected in the South Pacific will be much muted. To summarize, it is the overall pattern and direction of change in both records that is reminiscent of global changes, while the magnitude of the same change is a reflection of their relative location and basinal effect.

Another prominent feature of the  $\epsilon_{Nd}$  record in Site 607 is the unradiogenic spike immediately before MIS 22 (Figure 5.3). This extreme negative  $\epsilon_{Nd}$  value between MIS 27 and 25 has been associated with intense cratonic erosion/weathering via ice sheet interaction with old continental basement rocks surrounding the North Atlantic (Clark et al., 2006; Yehudai et al., 2021). However, this unradiogenic  $\epsilon_{Nd}$  spike is absent in U1541. This suggests that the Site 607 record is registering a local weathering pulse that is not propagated along the deep circulation pathway. Not only that this peak is absent in U1541, other equatorial and South Atlantic  $\epsilon_{Nd}$  time series

that cover the MPT do not exhibit this unradiogenic pulse either (Yehudai et al., 2021). Interestingly, there is no signature of enhanced cratonic erosion prior to MIS 16 or 36, the other two time periods when  $\epsilon_{Nd}$  excursions are observed in both records. Therefore, the unradiogenic peak in the Site 607 record appears to be a one-off episode of continental weathering and may not be particularly associated with the initiation of 100 kyr interglacial-glacial world

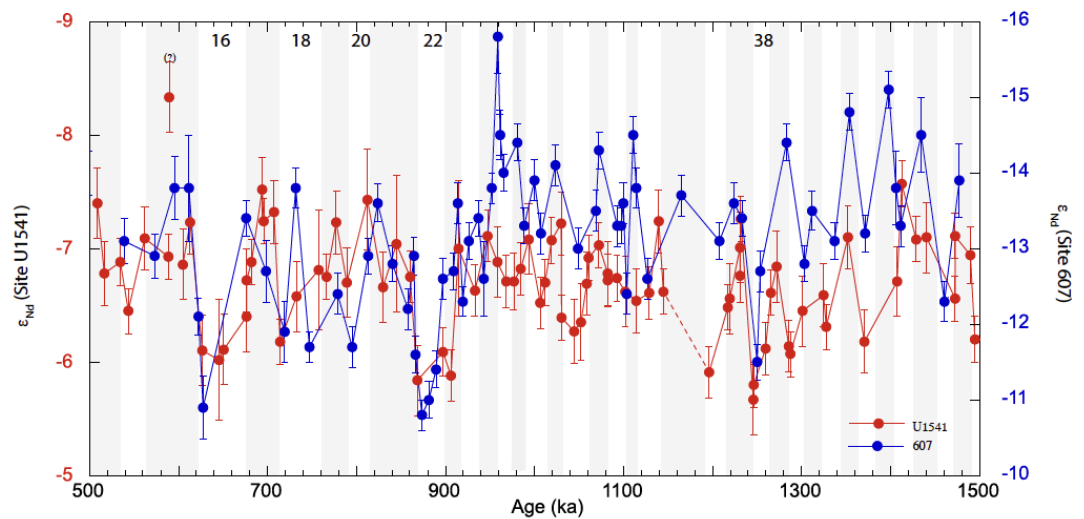


Figure 5.2: Comparison between North Atlantic (ODP 607) and South Pacific (U1541)  $\epsilon_{Nd}$  timeseries for covering 500-1500 ka. The grey bars and marine isotope stages represent the interglacial and glacial respectively. Core gap is shown as broken line. Measurement uncertainties ( $2\sigma$ ) are shown by vertical errors bars.

### 5.3 The $\epsilon_{Nd}$ and $\delta^{18}O$ records

The  $\epsilon_{Nd}$  record for site U1541 closely follows the trends of the global benthic oxygen isotope ( $\delta^{18}O_{calcite}$ , Fig. 5.3a) record by Ahn et al., 2017 and oxygen isotope

of seawater ( $\delta^{18}\text{O}_{\text{sw}}$ , Fig. 5.3b) record for the South Atlantic by Elderfield et al., 2012. Both records (Fig.5.2, a,b) display a similar sawtooth pattern as the climate fluctuates between glacial and interglacial periods. Both  $\delta^{18}\text{O}_{\text{calcite}}$  and  $\delta^{18}\text{O}_{\text{sw}}$  records show a shift towards higher values across glacial periods. The  $\epsilon_{\text{Nd}}$  record at U1541 follows a similar trend with  $\epsilon_{\text{Nd}}$  becoming more radiogenic during glacial periods. Further statistical analysis using a Pearson correlation test shows that while there is a correlation between both  $\delta^{18}\text{O}_{\text{calcite}}$  and  $\delta^{18}\text{O}_{\text{sw}}$  with  $\epsilon_{\text{Nd}}$ , across the MPT, the correlation between  $\delta^{18}\text{O}_{\text{calcite}}$  and  $\epsilon_{\text{Nd}}$  is stronger (Fig. 5.2). For this reason, we have chosen to use  $\delta^{18}\text{O}_{\text{sw}}$  as the primary proxy for comparison with the  $\epsilon_{\text{Nd}}$  record for site U1541.

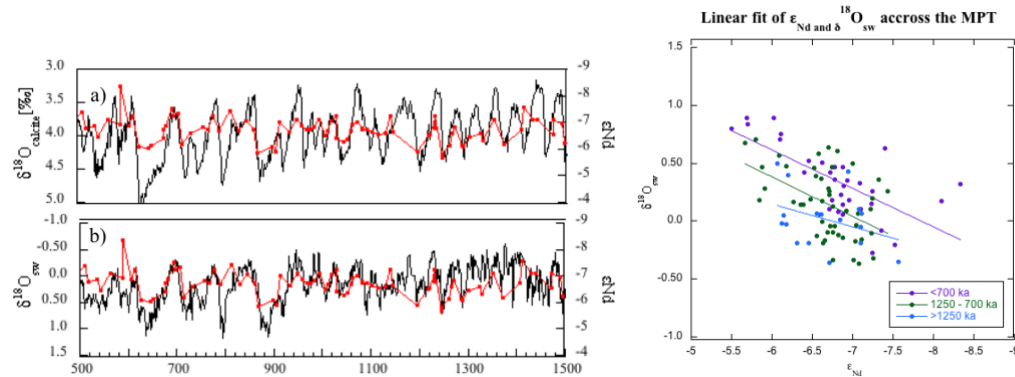


Figure 5.3: Proxy compilation showing  $\delta^{18}\text{O}$  compared to Nd isotopes for site U1541. a) Global benthic  $\delta^{18}\text{O}_{\text{calcite}}$  [‰] stack (Ahn et al., 2017) and b) Benthic  $\delta^{18}\text{O}_{\text{sw}}$  record from the South Atlantic Ocean (modified from Elderfield et al., 2012). Both with Nd isotopes ( $\epsilon_{\text{Nd}}$ , red). C) A linear model showing the correlation between  $\delta^{18}\text{O}_{\text{sw}}$  and  $\epsilon_{\text{Nd}}$ .

Thermodynamics suggests  $\delta^{18}O_{calcite}$  reflects changes in both ocean temperature and ice volume (Chappell and Shackleton, 1986; Ruddimen, 2007, Elderfield et al., 2012) while  $\delta^{18}O_{sw}$  isolates the ice volume component (LeGrande and Schmidt, 2006, Elderfield et al., 2012, Rohling, 2013) tracking changes in ice volume over the oceans. In comparison, variations in deep ocean  $\epsilon_{Nd}$  reflects end member mixing proportions of Atlantic and Pacific sourced waters. Both  $\epsilon_{Nd}$  and  $\delta^{18}O_{sw}$  variations follow changing climate conditions and show a strong correlation to one another with fluctuations in both occurring simultaneously across the MPT. The correlation between  $\epsilon_{Nd}$  and  $\delta^{18}O_{sw}$  appears to strengthen across the MPT becoming the most significant after the MPT has completed. This suggests there is a mechanistic link between ice volume and deep ocean circulation across the MPT.

#### **5.4 North vs. South Control**

The question of whether the Northern or Southern Hemisphere initiated and controlled the MPT has been a topic of debate in paleoceanography. New  $\epsilon_{Nd}$  timeseries from the central South Pacific provide an opportunity to revisit this question, particularly from a Southern Hemisphere perspective. Long-term cooling and Northern Hemisphere ice sheet growth began about 2.5 Ma (Raymo et al., 1989, 1994). However, a recent study by Tzedakis et al. (2017) showed that the Northern Hemisphere ice sheet did not reach a critical size until MIS 35-36, when it was able to survive consecutive summer insolation peaks without undergoing major melting (Fig. 5.1). This suggests that MIS 35-36 was the time interval when the size of the Northern

Hemisphere ice sheet began to play an important role in shifting Atlantic deep ocean circulation.

The first  $\epsilon_{Nd}$  excursion during MIS 38 in the U1541 record predates the first time the Northern Hemisphere survived an insolation peak or ice growth in Antarctica during MIS 22, as claimed by Elderfield et al. (2012). Raymo et al. (2006) suggested that at  $\sim 1$  Ma, Antarctic ice sheets transitioned from being terrestrial to becoming glaciomarine. In context of Antarctica, glaciomarine ice sheets are those that have reached the ocean. When glaciomarine ice sheets reach the oceans, they are heavily influenced by sea level and begin to calve ice sheets that melt in the oceans and produce Ice Rafted Debris (IRD). Therefore, we would expect IRD is an indicator of glacial advancement to the ocean. In contrast, land-based terrestrial Antarctic glaciers would retreat via surface melt that is highly dependent on summer heating. Based on this logic, it is reasonable to argue that the prominent peaks in IRD that begin around 1400 ka, could potentially mark the arrival of more consistent glaciomarine ice sheets across glacial cycles.

Site U1539 ( $56^{\circ}09'$  S,  $115^{\circ}08'$ W, water depth 4070 m), located south of Site U1541 on the Sub-Antarctic Front (SAF), is well-positioned to track IRD from iceberg melting off the Antarctic source (Fig. 2.1). The shipboard IRD flux record shows significant activity during early glacial periods beginning  $\sim 1400$  ka (Fig. 5.4) where larger peaks in IRD become more prominent. The largest peaks coincide with the

significant ocean circulation events at 1250 ka, 900 ka and 650ka suggesting these peaks are important. These changes in ice sheet dynamics have the potential to disrupt ocean circulation in ways that are similar to the changes we see in deep ocean circulation across the MPT and recent work has supported this.

Using a high-resolution IRD record from the South Atlantic, it has recently been shown that during glacial periods, iceberg melting at the SAF can suppress North Atlantic Deep Water (NADW) formation (Starr et al., 2021). This suggested mechanism aligns with our  $\epsilon\text{Nd}$  and IRD flux data, where IRD peaks between 1400-1200 ka is followed by  $\epsilon\text{Nd}$  excursions. Therefore, the effect of Antarctic ice sheet control in ushering the first disruption in deep ocean circulation cannot be ruled out. While additional supporting evidence would be necessary (such as source of IRD via provenance study) to firmly establish this claim, it is a reasonable working hypothesis that the Antarctic ice sheet initiated the first deep ocean disruption.

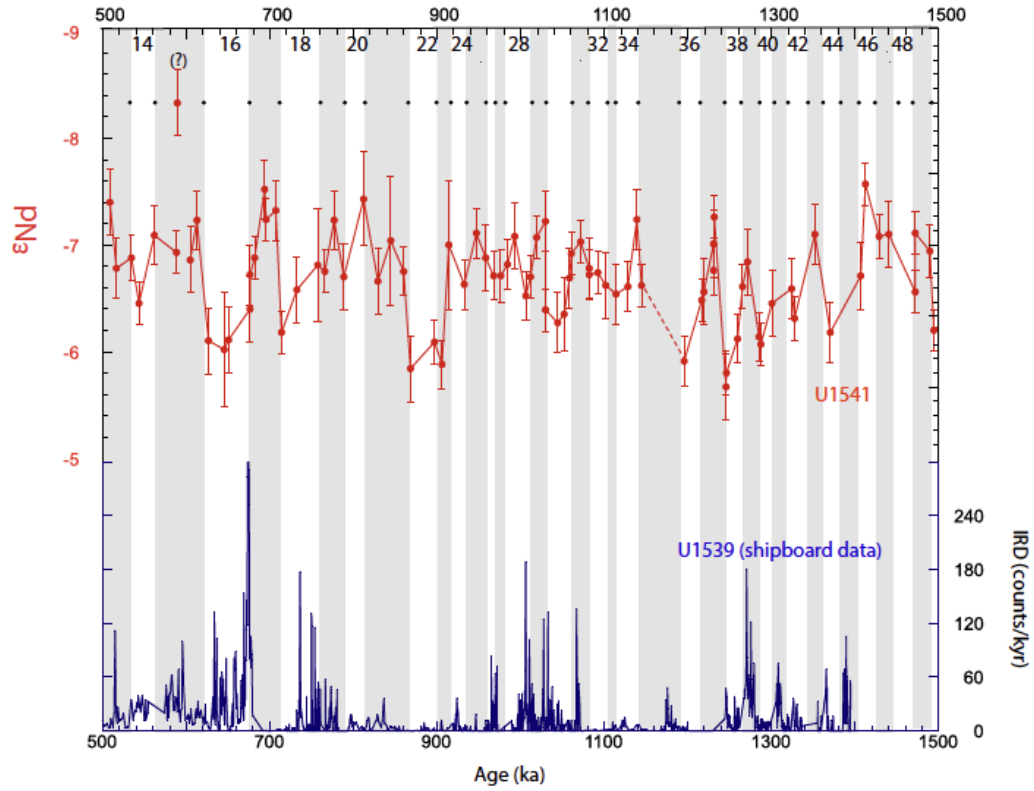


Figure 5.4: South Pacific  $\epsilon_{Nd}$  and flux of Ice Rafted Debris (U1539, shipboard data, Winckler et al., 2021) for 500-1500 ka. The grey bars and marine isotope stages represent the interglacial and glacial respectively. Core gap is shown as broken line. Measurement uncertainties ( $2\sigma$ ) are shown by vertical errors bars. Black dots are boundaries of Marine Isotope Stages (Lisiecki and Raymo, 2005).

## CONCLUSIONS

The Neodymium (Nd) isotope record for site U1541 is the first high resolution record for the South Pacific to encompass the entire period of the Mid-Pleistocene Transition (MPT, 1500-700 ka) therefore adding a Pacific perspective to existing literature. The Nd isotope record captures deep ocean circulation changes across the MPT through variations in ... More Pacific water influence (i.e., NPDW) is reflected through more radiogenic values and more Atlantic (i.e., NADW) through less radiogenic  $\epsilon_{Nd}$  values.

First, our record shows that deep ocean circulation changes across the MPT follow Earth's climate pacing illustrated by fluctuations in  $\epsilon_{Nd}$  across glacial periods, consistently reflecting increased Pacific water influence and weakened deep ocean circulation. Of these fluctuations, our record exposed three periods of near complete breakdown in MOC reflected through highly radiogenic  $\epsilon_{Nd}$  values at ~1250 ka, ~900 ka, and ~650 ka. These events correspond with other significant ice volume events. For example, the 1250 ka event corresponds to the first skipped interglacial discovered by Tedakis et al., 2017 where there was minor ice loss compared to previous interglacial periods. The presence of the 1250 ka event marks an important feature of our record as previous research has emphasized the importance of the 900 ka event. The discovery of the 1250 ka event and the cooccurrence of other important climatic events suggests this was an important period during the MPT and more attention should be focused on the events occurring at and around 1250 ka.

Second, the Nd isotope record for the South Pacific captures' global changes in deep ocean circulation. The agreement between the North Atlantic Nd isotope record by Kim et al (2021) and our South Pacific record is strong with minor differences between the two records that can be attributed to localized differences. The agreement between the two records suggests changes in deep ocean circulation were part of a global event.

Third, there is a strong correlation between deep ocean circulation changes beginning around 1250 ka and ice volume. This provides evidence that there is a link between deep ocean circulation and ice volume. Given the intrinsic relationship between deep ocean circulation and ice volume on climate, it is fair to assume both could have been components in a climate feedback loop where larger ice volume lead to weakened deep ocean circulation and further CO<sub>2</sub> drawdown and storage. The drawdown and storage of additional CO<sub>2</sub> would have allowed the earth to cool further and for the ice sheets to grow even larger with each consecutive glacial. We hypothesize that increased ice sheet growth over Antarctica resulted in a shift in these ice sheets from terrestrial to glaciomarine. Northern Hemisphere ice growth has commonly been believed to have played a significant role in the initiation of the MPT through the context of global changes in deep ocean circulation. However, our  $\epsilon_{Nd}$  record and IRD flux data for the Southern Pacific supports the role of Southern hemisphere ice growth on the initiation of the MPT. In such a transition, the calving and melting of icebergs from the parent ice sheet induced by ice sheet interaction with seawater in glaciomarine ice sheets would introduce large amounts of freshwater into the Southern Ocean portion of MOC, destabilizing the water column by suppressing

NADW formation. Such changes could cause deep ocean circulation changes similar to what we see in our record.

Therefore, we can conclude that the Nd isotope record for the South Pacific has successfully captured global changes in deep ocean circulation across the MPT. These changes follow Earth's global climate pacing and a feedback loop between Antarctic ice sheet growth and deep ocean circulation could have been a key contributor in solidifying the conditions of the MPT. More work still needs to be done to establish the control of Antarctic ice sheets on the MPT, the effects of Antarctic ice sheets in ushering the disruptions in deep ocean circulation seen in the record. However, the influence of Antarctic ice sheets in ushering the MPT cannot be ruled out as a potential mechanism for establishing the 100 ky glacial cycles of the MPT. This research has provided critical data to support this claim and fill the gaps in our knowledge of how deep ocean circulation in the South Pacific changes across the MPT and answer some critical questions as to why.

## REFERENCES

- Abbott, A. N., Haley, B. A., McManus, J., & Reimers, C. E. (2015a). The sedimentary flux of dissolved rare earth elements to the ocean. *Geochimica et Cosmochimica Acta*, 154, 186-200.
- Abbott, A. N., Haley, B. A., & McManus, J. (2015b). Bottoms up: Sedimentary control of the deep North Pacific Ocean's  $\epsilon\text{Nd}$  signature. *Geology*.
- Ahn, S., Khider, D., Lisiecki, L. E., & Lawrence, C. E. (2017). A probabilistic Pliocene–Pleistocene stack of benthic  $\delta^{18}\text{O}$  using a profile hidden Markov model. *Dynamics and Statistics of the Climate System*, 2(1), dzx002.
- Albarède, F., & Goldstein, S. L. (1992). World map of Nd isotopes in sea-floor ferromanganese deposits. *Geology*, 20(8), 761–763.
- Barker, S., Zhang, X., Jonkers, L., Lordsmith, S., Conn, S., & Knorr, G. (2021). Strengthening Atlantic Inflow Across the Mid-Pleistocene Transition. *Paleoceanography and Paleoclimatology*, 36(4).
- Basak, C., Pahnke, K., Frank, M., Lamy, F., & Gersonde, R. (2015). Neodymium isotopic characterization of Ross Sea Bottom Water and its advection through the southern South Pacific. *Earth and Planetary Science Letters*, 419, 211–221.
- Berger, A. (1988). Milankovitch Theory and climate. *Reviews of Geophysics*, 26(4), 624–657.

- Berger, W., & Jansen, E. (1994). Mid-Pleistocene Climate Shift - The Nansen Connection, 85.
- Broecker, W., & Peng, T. (1982). *Tracers in the Sea*. Lamont-Doherty Geological Observatory.
- Carter, P., Vance, D., Hillenbrand, C.D., Smith, J.A., & Shoosmith, D.R. (2012). The neodymium isotopic composition of waters masses in the eastern Pacific sector of the Southern Ocean. *Geochimica et Cosmochimica Acta*, 79, 41 - 59.
- Chalk, T. B., Hain, M. P., Foster, G. L., Rohling, E. J., Sexton, P. F., Badger, M. P. S., et al. (2017). Causes of ice age intensification across the Mid-Pleistocene Transition. *Proceedings of the National Academy of Sciences*, 114(50), 13114–13119.
- Clark, P. U., Archer, D., Pollard, D., Blum, J. D., Rial, J. A., Brovkin, V., et al. (2006). The middle Pleistocene transition: characteristics, mechanisms, and implications for long-term changes in atmospheric pCO<sub>2</sub>. *Quaternary Science Reviews*, 25(23–24), 3150–3184.
- Clark, P., & Pollard, D. (1998). Origin of the Middle Pleistocene Transition by ice sheet erosion of regolith.
- Elderfield, H., Ferretti, P., Greaves, M., Crowhurst, S., McCave, I. N., Hodell, D., & Piotrowski, A. M. (2012). Evolution of Ocean Temperature and Ice Volume Through the Mid-Pleistocene Climate Transition. *Science*, 337(6095), 704–709.
- Elmore, A. C., Piotrowski, A. M., Wright, J. D., & Scrivner, A. E. (2011). Testing the extraction of past seawater Nd isotopic composition from North Atlantic deep sea sediments and foraminifera. *Geochemistry, Geophysics, Geosystems*, 12(9).

- Farmer, J. R., Hönisch, B., Haynes, L. L., Kroon, D., Jung, S., Ford, H. L., et al. (2019). Deep Atlantic Ocean carbon storage and the rise of 100,000-year glacial cycles. *Nature Geoscience*, *12*(5), 355–360.
- Gutjahr, M., Frank, M., Stirling, C. H., Keigwin, L. D., & Halliday, A. N. (2008). Tracing the Nd isotope evolution of North Atlantic Deep and Intermediate Waters in the western North Atlantic since the Last Glacial Maximum from Blake Ridge sediments. *Earth and Planetary Science Letters*, *266*(1), 61–77.
- Hasenfratz, A. P., Jaccard, S. L., Martínez-García, A., Sigman, D. M., Hodell, D. A., Vance, D., et al. (2019). The residence time of Southern Ocean surface waters and the 100,000-year ice age cycle. *Science*, *363*(6431), 1080–1084.
- Hays, J. D., Imbrie, J., & Shackleton, N. J. (1976). Variations in the Earth's Orbit: Pacemaker of the Ice Ages. *Science, New Series*, *194*(4270), 1121–1132.
- Hönisch, B., Hemming, N. G., Archer, D., Siddall, M., & McManus, J. F. (2009). Atmospheric Carbon Dioxide Concentration Across the Mid-Pleistocene Transition. *Science*, *324*(5934), 1551–1554.
- Jacobsen, S. B., & Wasserburg, G. J. (1980). Sm-Nd Isotopic Systematics of Chondrites and Achondrites. *Meteoritics*, *15*(4), 307–307.
- Jeandel, C. (1993). Concentration and isotopic composition of Nd in the South Atlantic Ocean. *Earth and Planetary Science Letters*, *117*(3), 581–591.
- Johnson, G. C. (2008). Quantifying Antarctic Bottom Water and North Atlantic Deep Water volumes. *Journal of Geophysical Research: Oceans*, *113*(C5).

- Lamy, F., Winckler, G., & Alvarez Zarikian, C. A. (2021). *Volume 383: Dynamics of the Pacific Antarctic Circumpolar Current (DYNAPACC)*. (Expedition 383 Scientists, Ed.) (Vol. 383). International Ocean Discovery Program.
- Lear, C. H., Billups, K., Rickaby, R. E. M., Diester-Haass, L., Mawbey, E. M., & Sosdian, S. M. (2016). Breathing more deeply: Deep ocean carbon storage during the mid-Pleistocene climate transition. *Geology*, *44*(12), 1035–1038.
- LeGrande, A. N., & Schmidt, G. A. (2006). Global gridded data set of the oxygen isotopic composition in seawater. *Geophysical Research Letters*, *33*(12).
- Lin, L., Khider, D., Lisiecki, L. E., & Lawrence, C. E. (2014). Probabilistic sequence alignment of stratigraphic records. *Paleoceanography*, *29*(10), 976–989.
- Lisiecki, L. E., & Raymo, M. E. (2005). A Pliocene-Pleistocene stack of 57 globally distributed benthic  $\delta^{18}\text{O}$  records. *Paleoceanography*, *20*(1).
- Martin, E., & Haley, B. (2000). Fossil fish teeth as proxies for seawater Sr and Nd isotopes.
- Milankovitch, Milutin. (1941). *Canon of Insolation and the Ice-Age Problem* (1st ed.). Agency for Textbooks.
- Molina-Kescher, M., Frank, M., & Hathorne, E. C. (2014). South Pacific dissolved Nd isotope compositions, rare earth element and nutrient concentrations from SONNE cruise SO213 [Data set]. *Supplement to: Molina-Kescher, M et al. (2013): South Pacific dissolved Nd isotope compositions and rare earth element distributions: Water mass mixing versus biogeochemical cycling. Geochimica et Cosmochimica Acta*, *127*, 171-189.

- Palmer, M. R., & Elderfield, H. (1985). Variations in the Nd isotopic composition of foraminifera from Atlantic Ocean sediments. *Earth and Planetary Science Letters*, 73(2), 299–305.
- Pena, L., Goldstein, S., Hemming, S., Jones, K., Calvo, E., Pelejero, C., & Cacho, I. (2013). Rapid changes in meridional advection of Southern Ocean intermediate waters to the tropical Pacific during the last 30 kyr. *Earth and Planetary Science Letters*, 368, 20–32.
- Pena, L. D., & Goldstein, S. L. (2014). Thermohaline circulation crisis and impacts during the mid-Pleistocene transition. *Science*, 345(6194), 318–322.
- Piotrowski, A. M., Goldstein, S. L., Hemming, S. R., & Fairbanks, R. G. (2004). Intensification and variability of ocean thermohaline circulation through the last deglaciation. *Earth and Planetary Science Letters*, 225(1–2), 205–220.
- Piotrowski, A. M., Goldstein, S. L., Hemming, S. R., & Fairbanks, R. G. (2005). Temporal relationships of carbon cycling and ocean circulation at glacial boundaries. *Science (New York, N.Y.)*, 307(5717), 1933–1938.
- Piotrowski A.M., Galy, A., Nicholl, J.A.L., Roberts, N.L., Wilson, D.J., Clegg, J., and Yu, J., (2012), Reconstructing deglacial North and South Atlantic deep water source using foraminiferal Nd isotopes, *Earth and Planetary Science Letters* 357-358, 289-297.
- Pisias, N. G., & Moore, T. C. (1981). The evolution of Pleistocene climate: A time series approach. *Earth and Planetary Science Letters*, 52(2), 450–458.

- Poirier, R., & Billups, K. (2014). The intensification of northern component deepwater formation during the mid-Pleistocene climate transition. *Paleoceanography and Paleoclimatology*, 29(11).
- Raymo, M. E., Ruddiman, W. F., Shackleton, N. J., & Oppo, D. W. (1990). Evolution of Atlantic-Pacific  $\delta^{13}\text{C}$  gradients over the last 2.5 m.y. *Earth and Planetary Science Letters*, 97(3), 353–368.
- Raymo, M. E. (1997). The timing of major climate terminations. *Paleoceanography*, 12(4), 577–585.
- Raymo, M. E., Oppo, D. W., & McManus, J. F. (2004). Pleistocene Glaciation and the Stability of North Atlantic Thermohaline Circulation, 2004, PP13B-02. Presented at the AGU Fall Meeting Abstracts.
- Raymo, M. E., Lisiecki, L. E., & Nisancioglu, K. H. (2006). Plio-Pleistocene Ice Volume, Antarctic Climate, and the Global  $\delta^{18}\text{O}$  Record. *Science*, 313(5786), 492–495.
- Rickli, J., Gutjahr, M., Vance, D., Fischer-Gödde, M., Hillenbrand, C.-D., & Kuhn, G. (2014). Neodymium and hafnium boundary contributions to seawater along the West Antarctic continental margin. *Earth and Planetary Science Letters*, 394, 99–110.
- Roberts, N. L., Piotrowski, A. M., McManus, J. F., & Keigwin, L. D. (2010). Nd isotopes of sediments, foraminifera and fish debris of the western North Atlantic [Data set]. *Supplement to: Roberts, NL et al. (2010): Synchronous deglacial overturning and water mass source changes. Science*, 327(5961), 75-78, <https://doi.org/10.1126/science.1178068>. PANGAEA.

- Roberts, N. L., Piotrowski, A. M., Elderfield, H., Eglinton, T. I., & Lomas, M. W. (2012). Rare earth element association with foraminifera. *Geochimica et Cosmochimica Acta*, 94, 57–71.
- Rohling, E. J. (2013). PALEOCEANOGRAPHY, PHYSICAL AND CHEMICAL PROXIES | Oxygen Isotope Composition of Seawater. In *Encyclopedia of Quaternary Science* (pp. 915–922). Elsevier.
- Ruddiman, W. (2013). *Earth's Climate: Past and Future* (2nd ed.). New York: W.H. Freeman and Company.
- Rutberg, R., Hemming, S., & Goldstein, S. (2000). Reduced North Atlantic Deep Water flux to the glacial Southern Ocean inferred from neodymium isotope ratios. *Nature*, 405, 935–8.
- Shackleton, N. J., & Opdyke, N. D. (1977). Oxygen isotope and palaeomagnetic evidence for early Northern Hemisphere glaciation. *Nature*, 270(5634), 216–219.
- Shaw, H. F., & Wasserburg, G. J. (1985). Sm-Nd in marine carbonates and phosphates: Implications for Nd isotopes in seawater and crustal ages. *Geochimica et Cosmochimica Acta*, 49(2), 503–518.
- Snyder, C. W. (2016). Evolution of global temperature over the past two million years. *Nature*, 538(7624), 226–228.
- Sosdian, S., & Rosenthal, Y. (2009). Deep-Sea Temperature and Ice Volume Changes Across the Pliocene-Pleistocene Climate Transitions. *Science*, 325(5938), 306–310.

- Starr, A., Hall, I. R., Barker, S., Rackow, T., Zhang, X., Hemming, S. R., et al. (2021). Antarctic icebergs reorganize ocean circulation during Pleistocene glacials. *Nature*, 589(7841), 236–241.
- Tachikawa, K., Jeandel, C., & Roy-Barman, M. (1999). A new approach to the Nd residence time in the ocean: the role of atmospheric inputs. *Earth and Planetary Science Letters*, 170(4), 433–446.
- Tachikawa, K., Rapuc, W., Dubois-Dauphin, Q., Guihou, A., & Skonieczny, C. (2020). Reconstruction of Ocean Circulation Based on Neodymium Isotopic Composition: Potential Limitations and Application to the Mid-Pleistocene Transition. *Oceanography*, 33(2), 80–87.
- Talley, L., Pickard, G., Emery, W., & Swift, J. (2011). *Descriptive Physical Oceanography* (6th ed.). Elsevier Ltd.
- Talley, L. (2013). Closure of the Global Overturning Circulation Through the Indian, Pacific, and Southern Oceans: Schematics and Transports. *Oceanography*, 26(1), 80–97.
- Tillinger, D. (2011). Physical oceanography of the present day Indonesian Throughflow. *Geological Society, London, Special Publications*, 355(1), 267–281.
- Tzedakis, P. C., Crucifix, M., Mitsui, T., & Wolff, E. W. (2017). A simple rule to determine which insolation cycles lead to interglacials. *Nature*, 542(7642), 427–432.
- Tziperman, E., & Huybers, P. (2008). Integrated Summer Insolation Forcing and 40,000-Year Glacial Cycles: The Perspective from an Ice-Sheet/Energy-Balance Model. *Paleoceanography*, 23.

- White, W. M. (2015). *Isotope Geochemistry*. John Wiley & Sons Ltd.
- Wilson, D. J., Piotrowski, A. M., Galy, A., & McCave, I. N. (2012). A boundary exchange influence on deglacial neodymium isotope records from the deep western Indian Ocean. *Earth and Planetary Science Letters*, 341–344, 35–47.
- Wright, J. R. S., Seymour, H. F., Shaw, R. E., & Nd isotopes in conodont apatite: Variations with geological age and depositional environment. *Geological Society of America Special Paper* **196**, 325-340 (1984).
- Wu, Y., Pena, L. D., Anderson, R. F., Hartman, A. E., Bolge, L. L., Basak, C., et al. (2022). Assessing neodymium isotopes as an ocean circulation tracer in the Southwest Atlantic. *Earth and Planetary Science Letters*, 599, 117846.
- Yehudai, M., Kim, J., Pena, L. D., Jaume-Seguí, M., Knudson, K. P., Bolge, L., et al. (2021). Evidence for a Northern Hemispheric trigger of the 100,000-y glacial cyclicity. *Proceedings of the National Academy of Sciences*, 118(46).
- Kawabe, M., & Fujio, S. (2010). Pacific Ocean Circulation Based on Observation. *Journal of Oceanography*, 66, 389–403.
- Kim, J., Goldstein, S. L., Pena, L. D., Jaume-Seguí, M., Knudson, K. P., Yehudai, M., & Bolge, L. (2021). North Atlantic Deep Water during Pleistocene interglacials and glacials. *Quaternary Science Reviews*, 269, 107146.
- Kominz, M. A., & Pisias, N. G. (1979). Pleistocene Climate: Deterministic or Stochastic? *Science*, 204(4389), 171–173.